Atomic-Scale Variations of the Tunneling Distribution in a Scanning Tunneling Microscope Observed by Ballistic-Electron-Emission Microscopy

H. Sirringhaus, E. Y. Lee, and H. von Känel

Laboratorium für Festkörperphysik, Eidgenössische Technische Hochschule Hönggerberg, CH-8093 Zürich, Switzerland

(Received 28 December 1994)

In situ ballistic-electron-emission microscopy (BEEM) and spectroscopy (BEES) have been performed at 77 K on epitaxial $CoSi_2$/Si (100) and (111). BEEM images reflect the atomic-scale periodicity of the surface topography. Atomically resolved BEES is correlated with tunneling spectroscopy and the apparent tunneling barrier height. The effect is due to variations of the energy distribution of the tunneling electrons on an atomic scale.

PACS numbers: 61.16.Ch, 73.20.At, 73.40.Gk, 73.40.Ns

Various mechanisms have been invoked to explain atomic resolution in scanning tunneling microscopy (STM). On semiconducting or highly corrugated metal surfaces STM topographs are adequately interpreted in terms of spatial variations of the local density of states (LDOS) penetrating through the laterally uniform potential barrier into the vacuum [1]. It is still a matter of debate to what extent tip-sample interactions contribute to the observed atomic corrugation, in particular on close-packed metal surfaces [2]. They give rise to a redistribution of charge in the presence of the tip and a site dependence of the tunneling barrier [3].

Valuable information about the resolution mechanism may be contained in the energy and momentum distribution of the sample states contributing to the tunneling current I_t, which might in principle vary on an atomic scale. In ordinary STM the tunneling distribution is only accessible to a limited extent in the spectroscopy mode, because only the total I_t can be measured. However, if the sample is a thin metal film on top of a semiconducting substrate, ballistic-electron-emission microscopy (BEEM) and spectroscopy (BEES) [4] can be performed. BEEM is based on a STM as well, but in addition to I_t one measures the current due to those carriers which are able to cross the Schottky barrier at the buried metal-semiconductor (M-S) interface. BEEM has been very successful in the study of hot carrier interface transport [5]. Moreover, the BEEM current is sensitive to the injected tunneling distribution, such that one might hope to use BEEM also as an "energy and momentum analyzer" for the carriers injected by an STM tip. Here we report on the first direct observation of atomic-scale variations of the tunneling distribution by BEEM. The samples were metallic $CoSi_2$ films grown by molecular beam epitaxy (MBE) on n-Si (100) and on Si (111) of both doping types [6,7]. The BEEM experiments were preformed *in situ* at 77 K in a low-temperature UHV STM [7]. Chemically etched tungsten tips were cleaned in the STM chamber by Ar sputtering.

On Si-rich $CoSi_2$/Si (100) two surface phases coexist [6]: a $\sqrt{2} \times \sqrt{2}R45°$ reconstruction (abbreviated by $\sqrt{2}$) with a square arrangement of the topmost Si atoms [lower right in Fig. 1(a)] and a $3\sqrt{2} \times \sqrt{2}R45°$ reconstruction ($3\sqrt{2}$). On the latter two neighboring atomic [100] rows are shifted by $(a/2)[100]$ ($a = 5.43$ Å), whereas every third row remains in the position corresponding to the $\sqrt{2}$ reconstruction [6]. In contrast to close-packed metal surfaces [2] the $CoSi_2$ surface can be atomically resolved in STM up to relatively high tip voltages ($V_t = -1.5$ V in this case). This enables us to record simultaneously an atomic-resolution STM topograph and the corresponding BEEM image [Fig. 1(b)]. Most strikingly, the BEEM image also reflects the atomic surface periodicity. The BEEM current is smaller by (10–20)% on the topographic maxima than on the minima. On the $\sqrt{2}$ reconstruction the average BEEM current is larger than on the shifted double rows of the $3\sqrt{2}$ reconstruction. Surface point defects like the missing adatom indicated by the arrow also increase the BEEM current [7]. Since I_t is kept constant during the acquisition of the BEEM image [8], the contrast can only be interpreted as the first direct observation of variations of the STM tunneling distribution on an atomic scale.

In the following it will be shown that atomically resolved BEES in the constant current (CC) mode $[I_B(V_t)_{I_t=\text{const}}]$ is clearly correlated with conventional tunneling spectroscopy as a function of voltage $[I_t(V_t)_{z=\text{const}}]$ and tip-to-sample separation $[I_t(z)_{V_t=\text{const}}]$. From the $I_t(V_t)$ spectra the normalized conductivity $(dI_t/dV_t)/(I_t/V_t) \propto$ LDOS has been calculated [9]. The $I_t(z)$ spectra yield a value for the apparent tunneling barrier height $\Phi(V_t)$ [10]. All BEES spectra set in at the Schottky barrier height on Si (100) of 0.72 ± 0.05 V [11].

Let us first consider the atomic resolution on the $\sqrt{2}$ reconstruction. The BEES contrast [Fig. 2(a)] becomes visible above ~ -1 V, with the current being lower on the topograhic maxima [see Fig. 1(b)]. It disappears above ~ -2.3 V. By that voltage the atomic resolution on the $\sqrt{2}$ reconstruction in STM has also been lost. In the corresponding LDOS spectra (not shown) there is no indication of a site-specific feature which could be responsible for the BEEM contrast. Instead, we observe a characteristic difference in the $I_t(V_t)$ spectra [Fig. 2(b)]: The voltage

0031-9007/95/74(20)/3999(4)$06.00

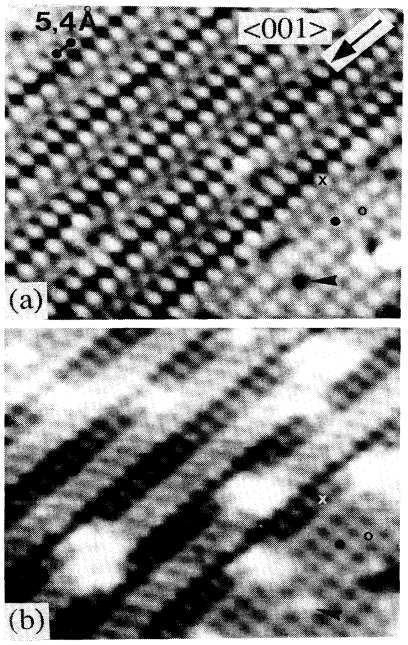

FIG. 1. STM topograph (a) and simultaneously recorded forward BEEM image (b) on the Si-rich $CoSi_2/n$-Si (100) surface ($V_t = -1.5$ V, $I_t = 3$ nA, film thickness $d = 38$ Å). The center part displays a $3\sqrt{2} \times \sqrt{2}R45°$ reconstruction, whereas the lower right is $\sqrt{2} \times \sqrt{2}R45°$ reconstructed. The $\sqrt{2}$ topographic corrugation is 0.15 Å. The BEEM contrast ranges from 25 pA (black) to 55 pA (white).

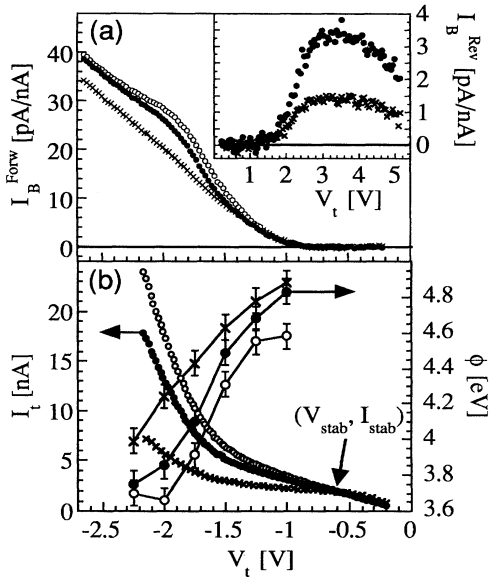

FIG. 2. (a) BEES spectra $I_B(V_t)_{I_t=\text{const}}$ ($I_t = 3$ nA) normalized to a tunneling current of 1 nA. The spectra were taken on the surface of Fig. 1 at every point of an atomic-resolution STM topograph and averaged over equivalent sites in the surface unit cell. The filled (open) circles belong to the $\sqrt{2}$ corrugation maxima (minima), the crosses to the $3\sqrt{2}$ maxima, as indicated in Fig. 1. The inset shows spatially averaged reverse BEES spectra ($I_t = 5$ nA, $d = 30$ Å) on the $3\sqrt{2}$ (crosses) and the $\sqrt{2}$ (filled circles) [compare Fig. 3(b)]. (b) (left scale) Corresponding tunneling spectra $I_t(V_t)_{z=\text{const}}$, stabilized at $V_{stab} = -0.6$ V, $I_{stab} = 2$ nA, and (right scale) apparent barrier height $\Phi(V_t)$, extracted from $I_t(z)_{V_t=\text{const}}$ spectra ($I_{stab} = 1$ nA). The symbols are the same as in (a).

dependence is more pronounced on the topographic minima than on the maxima, i.e., $I_t^{min} \gtrless I_t^{max}$ for all $|V_t| \gtrless |V_{stab}|$. This is true no matter at which voltage the tip is stabilized. Furthermore, $\Phi(V_t)$ is smaller by typically 0.2 eV on the topographic minima than on the maxima, for both negative [Fig. 2(b)] and positive voltages.

The average BEEM contrast between $\sqrt{2}$ and $3\sqrt{2}$ reconstructions sets in at ~ -1.4 V [Fig. 2(a)], but it remains visible up to at least -6 V. At such high voltages, where atomic resolution is no longer obtained in STM, the $3\sqrt{2}$ reconstruction can still be distinguished from the $\sqrt{2}$ reconstruction in topography because the $3\sqrt{2}$ reconstruction areas appear depressed by $\sim$0.2–0.4 Å relative to the $\sqrt{2}$ ones. This apparently electronic contrast at higher voltages, which is already faintly visible in Fig. 1(a), results in a smaller tip-to-sample separation on the $3\sqrt{2}$ reconstruction. A clear distinction between the two surfaces is also seen in $\Phi(V_t)$. On the $3\sqrt{2}$ reconstruction the value of Φ exceeds that on the $\sqrt{2}$ reconstruction above ~ -1.2 V [Fig. 2(b)]. Note that a larger tunneling barrier implies a smaller tip-to-sample separation.

We have also performed BEEM in a scattering spectroscopy mode [5]. By changing the polarity of the voltage ($V_t > 0$) holes are injected into the sample. In the metal they can create electron-hole pairs by scattering. The fraction of secondary electrons which is able to cross the interface is measured as the so-called reverse BEEM current. It has the same sign as the forward current discussed above. Figure 3 displays a STM topograph and reverse BEEM image of a $\sqrt{2}/3\sqrt{2}$ surface region. Also in reverse BEEM atomic resolution is obtained. The average reverse BEEM current is smaller on the $3\sqrt{2}$ surface, as in forward BEEM. However, the atomic variations of the reverse current on the $\sqrt{2}$ surface are in phase, rather than out of phase, with the topographic corrugation. Reverse BEES spectra on the $3\sqrt{2}$ and $\sqrt{2}$ surfaces are shown in the inset of Fig. 2(a). The very strong contrast remains visible up to the highest voltages.

One of the central questions is whether the contrast is mainly due to variations of the energy or the momentum distribution. In the following, it is argued that the energy distribution is the dominant cause of both the reverse and forward BEEM contrast.

(1) Reverse BEEM is primarily sensitive to the *energy* distribution, because only hot holes with energies $E^{hole} < E_F - \Phi_B$ can contribute. The broader the energy distribution is, the larger the reverse BEEM current. Since, at least at high energies, most secondary electrons are generated in the $CoSi_2$ metal [12], and their distribution is only

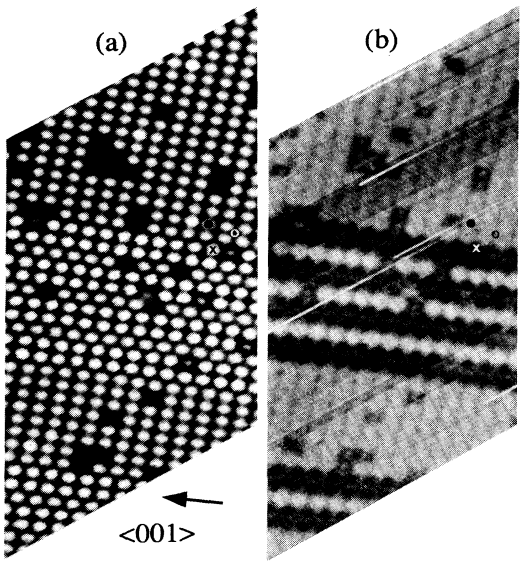

FIG. 3. STM topograph (a) and reverse BEEM image (b) on a similar $3\sqrt{2}/\sqrt{2}$ surface region ($V_t = 2$ V, $I_t = 10$ nA, $d = 38$ Å). The BEEM contrast ranges from 5 pA (black) to 12 pA (white).

weakly angle dependent [5], a strong dependence of the reverse BEEM current on the momentum distribution of the primary electrons is not expected. Therefore a strong reverse BEEM contrast is more likely to be related to the energy distribution.

(2) The $3\sqrt{2}/\sqrt{2}$ forward BEEM contrast remains up to at least -6 V. For $V_t \leq -4$ V, the BEEM current on n-Si (111) is no longer sensitive to the momentum distribution [7]. A similar behavior is expected for Si (100). This is so because at high energies all states in the interface Brillouin zone (IBZ) become available with nearly equal interface transmission probability, whereas at low voltages the BEEM current is restricted to small phase space volumes, the so-called critical angle cones [5], around the projected Si conduction band minima (CBM). Therefore, in forward BEEM, at least the high-voltage contrast must stem from the energy distribution.

(3) We have performed similar measurements on $CoSi_2$/n-Si (111), where a 2×1 surface reconstruction exists. On the 2×1, the forward BEEM current again varies out of phase with the topographic corrugation; i.e., the atomic-scale contrast is not reversed between Si (100) and (111). A reversal would, however, be expected if the contrast was related to the momentum distribution. It has been shown that, as a consequence of $k_\parallel$ conservation at epitaxial $CoSi_2$ and $NiSi_2$/Si (111) interfaces [7,13], a broadening of the momentum distribution results in an increase of the BEEM current, whereas on Si (100) a decrease is expected. This is so because on Si (111) the projected CMB's are not in the center of the IBZ, while for Si (100) they are. Note that for *both* interfaces the forward BEEM current is expected to be larger the sharper the energy distribution, because the BEEM spectra increase monotonically with voltage. On Si (111) a very similar correlation between BEEM, $\Phi(V_t)$, and the $I_t(V_t)$ spectra has been observed [11]. This similarity between two different surface structures suggests that the phenomena in BEEM and tunneling spectroscopy reported here are general phenomena of tunneling on an atomic scale, i.e., not related to any pathological feature of the specific surface electronic structure.

We conclude that change of the momentum distribution by itself cannot cause some of the salient features of the observed BEEM contrast. This does not exclude some contribution to the contrast from the angular distribution [11], but it strongly indicates that variations of the energy distribution dominate in both reverse and forward BEEM. Therefore, for a qualitative discussion, we focus on the energy distribution and show that a consistent explanation can be obtained on the basis of the relationship between the energy distribution and the tunneling barrier height.

Although one has to be careful in interpreting the measured $\Phi(V_t)$ in terms of the metal work function [10], different surface reconstructions usually do exhibit different work functions. This is due to charge transfer into surface states, changing the surface dipole. If this was the cause for the difference of Φ on the $\sqrt{2}$ and $3\sqrt{2}$ surfaces, the charge transfer would have to depend on the polarity of the applied field, because for $V_t > 0$ the $3\sqrt{2}$ surface exhibits a slightly smaller rather than larger tunneling barrier. However, this difference is smaller ($\Delta\Phi < 0.2$ eV), and can only be observed under favorable conditions. Correspondingly, for $V_t > 0$ the tip-to-sample separation z is larger on the $3\sqrt{2}$ surface by typically 0.2 Å. In planar tunneling theory the width $\Delta E_{1/e}$ of the energy distribution is determined by Φ and z according to $\Delta E_{1/e} \simeq (\hbar/\sqrt{2m})(\sqrt{\Phi}/z) \propto \Phi$ ($\sqrt{\Phi}\, z \simeq$ const in the CC mode). Therefore due to the sign change of $\Delta\Phi$ with the polarity of the tip the energy distribution is broader on the $3\sqrt{2}$ surface for $V_t < 0$, but sharper for $V_t > 0$. This explains why the $3\sqrt{2}$ current is smaller in both forward and reverse BEEM.

In contrast, the variation of Φ on the $\sqrt{2}$ surface is certainly not related to the work function, which, by definition, cannot vary on an *atomic* scale. Larger values of Φ on the corrugation maxima [14] can be explained within the Tersoff-Hamann (TH) theory [4]. In a simplified extension to finite voltages [15] the tunneling current is given by $I_t \propto \int_{E_F}^{E_F - eV_t} dE\, \rho_s(\vec{r}, E)$ ($\rho_{\text{tip}} = \text{const}$). The LDOS of the sample has the shape $\rho_s(\vec{r}, E) = C_1(E)e^{-2\kappa z} + C_2(E)e^{-2\gamma z}\cos[(\pi/a)x]^2$ ($\kappa = \sqrt{[2m(\Phi + E_F - eV_t/2 - E)]/\hbar^2}$, $\gamma = \sqrt{\kappa^2 + \pi^2/a^2}$, and a is the surface periodicity in the x direction). The effective barrier height on the corrugation maxima ($x = 0$) is larger because the states on the edge of the

Brillouin zone, which contribute to the second term, decay more rapidly into the vacuum ($\gamma > \kappa$). This results in a broader energy distribution on the maxima, for both negative and positive voltages, which explains the out-of-phase (in-phase) shift between forward (reverse) BEEM and topography. A broader energy distribution gives rise to a smaller forward and a larger reverse BEEM current.

The stronger voltage dependence of the $I_t(V_t)$ spectra on the topographic minima [Fig. 2(b)] is an interesting phenomenon in itself. It is equivalent to saying that the topographic corrugation on the $\sqrt{2}$ surface for a *fixed* z, i.e., for stabilization parameters (V_t, I_t) along an $I_t(V_t)$ spectrum, is smaller the larger $|V_t|$, which is indeed observed in STM topographs. Within the TH model this is explained by the voltage dependence of the transmission probability through the vacuum barrier, which is weaker the higher the barrier.

In spite of the nice correlation between BEEM and the measured $\Phi(V_t)$, on the basis of which we can qualitatively explain the BEEM data on Si (100) and Si (111), one has to be cautious in drawing any quantitative conclusions. From the above planar tunneling dependence of $\Delta E_{1/e}$ on the measured $\Phi(V_t)$, we estimate the difference of the energy width to be $\simeq$5% between maxima and minima on the $\sqrt{2}$ surface, and (10–15)% between the $\sqrt{2}$ and $3\sqrt{2}$ surfaces. These values have been used to calculate the BEEM current in the effective-mass, kinematic BEEM theory [5,16]. A significant surface contrast is thus obtained. However, the contrast is smaller than the experimental one by a factor of typically 2–5, in particular for reverse BEEM. Hence, other mechanisms might give rise to an anomalously large variation of the energy distribution compared to the one expected from planar tunneling [17]. As examples we mention a site-dependent loss of ballistic carriers by inelastic surface recombination or tip-sample interaction [3] affecting the potential profile experienced by the tunneling electrons and the "tunneling area," i.e., the lateral confinement of I_t.

In conclusion, the surface contrast in forward and reverse BEEM can be qualitatively explained by atomic-scale variations of the energy distribution of the injected carriers induced by variations of the tunneling barrier. A quantitative understanding, however, requires a careful, theoretical analysis, which we hope to stimulate. It might shed light on possible contributions from other mechanisms. The remarkable strength of the observed BEEM contrast might be a test criterion for theories of STM resolution on metals. This shows that BEEM cannot only be used to study hot carrier interface transport, but also to obtain information about the tunneling process at the surface, complementary to the one accessible with STM.

We gratefully acknowledge valuable discussions with A. Baratoff, contributions from U. Kafader, N. Onda, and C. Schwarz, and financial support from the Swiss National Science Foundation (Grant No. NFP 24), and the Swiss Research Foundation.

[1] J. Tersoff and D. R. Hamann, Phys. Rev. B **31**, 805 (1985).
[2] J. Wintterlin *et al.*, Phys. Rev. Lett. **62**, 59 (1989).
[3] S. Ciraci *et al.*, Phys. Rev. B **46**, 10411 (1992).
[4] L. D. Bell and W. J. Kaiser, Phys. Rev. Lett. **61**, 2368 (1988).
[5] L. D. Bell and W. J. Kaiser, in *Scanning Tunneling Microscopy,* edited by J. A. Stroscio and W. J. Kaiser (Academic Press, New York, 1993), p. 307.
[6] R. Stalder *et al.*, Surf. Sci. **271**, 355 (1992).
[7] H. Sirringhaus, E. Y. Lee, and H. von Känel, J. Vac. Sci. Technol. B **12**, 2629 (1994); Phys. Rev. Lett. **73**, 577 (1994).
[8] To prove that the BEEM contrast is not an artifact, we have measured I_t explicitly during the acquisition of the BEEM image with an additional analog-digital converter. The corresponding I_t image is uniform; i.e., there are no variations of I_t that could be induced by too high a scan speed. Using different scan speeds had no effect on the BEEM contrast. Furthermore, quantitatively the same contrast was observed in the spectroscopy mode (see Fig. 2).
[9] J. A. Stroscio, R. M. Feenstra, and A. P. Fein, Phys. Rev. Lett. **57**, 2579 (1986).
[10] H. Rohrer, in *Scanning Tunneling Microscopy and Related Methods,* edited by R. J. Behm (Kluwer, Dordrecht, 1990), p. 1.
[11] H. Sirringhaus, E. Y. Lee, and H. von Känel (to be published).
[12] E. Y. Lee *et al.* (to be published).
[13] A. Fernandez *et al.*, Phys. Rev. B **44**, 3428 (1991).
[14] R. Schuster *et al.*, Ultramicroscopy **42–44**, 533 (1992).
[15] N. D. Lang, Phys. Rev. B **34**, 5947 (1986).
[16] In planar tunneling a sharper energy distribution results in a sharper momentum distribution as well, which is taken into account for the quantitative analysis.
[17] Moreover, the experimental $I_t(V_t)$ spectra can only be simulated with the TH model by assuming a variation of $\Delta E_{1/e}$ larger than the one estimated from the measured difference of Φ.

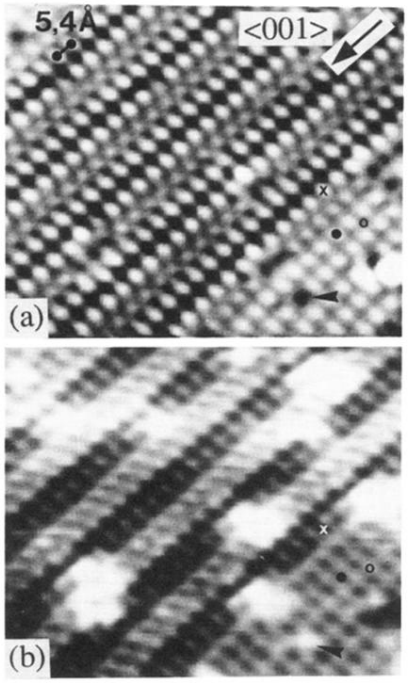

FIG. 1. STM topograph (a) and simultaneously recorded forward BEEM image (b) on the Si-rich $CoSi_2/n$-Si (100) surface ($V_t = -1.5$ V, $I_t = 3$ nA, film thickness $d = 38$ Å). The center part displays a $3\sqrt{2} \times \sqrt{2}R45°$ reconstruction, whereas the lower right is $\sqrt{2} \times \sqrt{2}R45°$ reconstructed. The $\sqrt{2}$ topographic corrugation is 0.15 Å. The BEEM contrast ranges from 25 pA (black) to 55 pA (white).

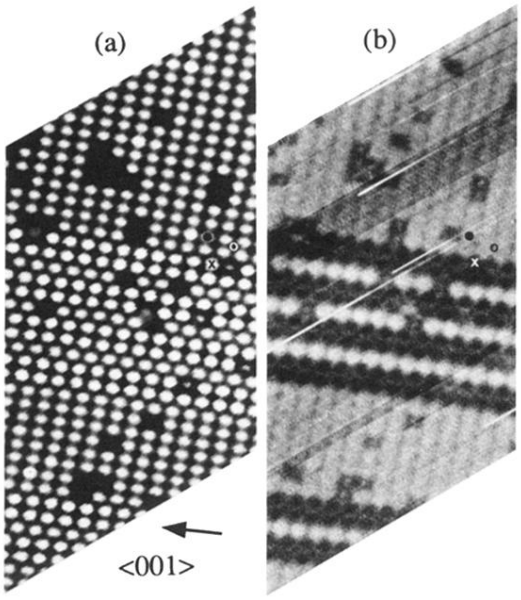

FIG. 3. STM topograph (a) and reverse BEEM image (b) on a similar $3\sqrt{2}/\sqrt{2}$ surface region ($V_t = 2$ V, $I_t = 10$ nA, $d = 38$ Å). The BEEM contrast ranges from 5 pA (black) to 12 pA (white).